Chapter 1
Supramolecular Self-assembled Nanomaterials for Fluorescence Bioimaging

Lei Wang and Guo-Bin Qi

Abstract In recent years, the construction of self-assembled nanomaterials with diversified structures and functionalities via fine tune of supramolecular building blocks increases rapidly. The self-assembled nanomaterials are potential high-efficient probes/contrast agents for high-performance fluorescence imaging techniques, which show distinguished advantages in terms of the availability of biocompatible imaging agents, maneuverable instruments, and high temporal resolution with good sensitivity. Generally, the self-assembled nanomaterials show high stability in vivo, prolonged half-life, and desirable targeting properties. Furthermore, self-assembled nanomaterials can be modulated by intelligent stimuli due to the dynamic nature of supramolecular materials. In this chapter, we will summarize recent advances in smart self-assembled nanomaterials as fluorescence probes/contrast agents for biomedical imaging, including long-term imaging, enzyme activity detection, and aggregation-induced retention (AIR) effect for diagnosis and therapy. The self-assembled nanomaterials will be classified into two groups, i.e., the ex situ and in situ self-assembled nanomaterials based on the assembly mode and the strategy for fluorescence regulation. Finally, we conclude with an outlook toward future developments of self-assembled nanomaterials for fluorescence bioimaging.

Keywords Supramolecular · Nanomaterials · Fluorescence bioimaging
In situ self-assembly

L. Wang (✉) · G.-B. Qi
CAS Center for Excellence in Nanoscience, CAS Key Laboratory for Biomedical Effects of Nanomaterials and Nanosafety, National Center for Nanoscience and Technology (NCNST), No. 11 Beiyitiao, Zhongguancun, Haidian District, Beijing 100190, China
e-mail: wanglei@nanoctr.cn

G.-B. Qi
e-mail: qigb@nanoctr.cn

H. Wang and L.-L. Li (eds.), *In Vivo Self-Assembly Nanotechnology for Biomedical Applications*, Nanomedicine and Nanotoxicology,
https://doi.org/10.1007/978-981-10-6913-0_1

1.1 Introduction

Inspired by sophisticated biological structures and their physiological processes, supramolecular chemistry inherits the spontaneous self-assembly of building blocks from their natural counterparts, which is driven by a variety of noncovalent interactions. Since the Nobel Prize was awarded to Lehn, Cram, and Pedersen for their pioneering works on guest-host and supramolecular chemistry in 1987, [1] supramolecular material science has undergone significant expansion. A large amount of materials self-assembled from functional building blocks through noncovalent interactions, such as hydrogen bonding, π−π, hydrophobic interactions, were designed and prepared, the structures and properties of which could be regulated by internal/external stimuli [2, 3]. Meanwhile, by emerging the modern nanoscience and biotechnology, a new research field of supramolecular nanomaterials has been gradually developed and attracted wide attention for biomedicine. Besides the traditional pre-organized nanomaterials prepared in solution, the in situ construction of self-assembled nanomaterials in vivo becomes a promising research field facing the structure evolution of self-assembled nanomaterials at biointerfaces.

Fluorescence is the emission of light from any substance and occurs from electronically excited states. In excited singlet states, the electron in the excited orbital is paired (by opposite spin) to the second electron in the ground-state orbital. Consequently, return to the ground state is spin allowed and occurs rapidly by emission of a photon. Based on the fluorescence phenomena and mechanism, fluorescence imaging technique enables highly sensitive, less-invasive, cheap, and safe detection using readily available instruments without requirements for the expense and difficulty of handling radioactive tracers for most biochemical measurements [4, 5]. To achieve desired signal output and high signal-to-noise ratio, a variety of fluorescent nanoprobes/contrast agents have been explored and attracted increasing attention for fluorescence imaging. To date, various fluorescent probes/contrast agents based on organic/polymeric nanomaterials have been developed for in vitro/in vivo imaging, which show negligible toxicity and superior capacity to combine multiple modalities on one nanomaterial. Furthermore, supramolecular self-assembled nanomaterials show outstanding advantages of high sensitivity and deep insight for in vivo processes [6, 7]. In this chapter, the fluorescent self-assembled nanomaterials were divided into ex situ construction in solution and in situ construction in vivo (Fig. 1.1). For ex situ nanoassemblies, great efforts should be paid for the preparation of defined superstructures and functionalities with specific supramolecular interactions. For in situ construction of self-assembled nanomaterials in living systems, we will focus on sophisticated responsiveness under physiological/pathological conditions to accomplish diagnosis and/or therapy of diseases in vitro and in vivo.

Generally, the isolated organic molecules in dilute solution are utilized to measure the fluorescence without intermolecular interactions. However, for most organic dyes, many of them in the supramolecular nanomaterials as nanoprobes/contrast agents are actually in the condensed state as well as a reduction in

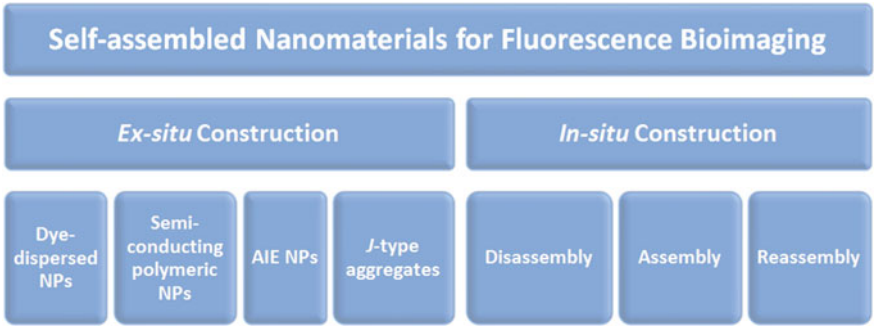

Fig. 1.1 Different classes of self-assembled nanomaterials for fluorescence bioimaging

fluorescence by aggregation-caused quenching (ACQ), [8] which is different from that in dilute solution. That is, supramolecular fluorescence nanomaterials usually show weakened or quenched fluorescence due to the ACQ effect, where the significant collisional quenching occurs between the fluorescence molecules. To address this issue, the supramolecular fluorescence nanomaterials should be designed and prepared by dispersing organic dyes down to a level avoiding concentration quenching in the nanomatrix or introducing bulky groups to prevent the aggregation [9, 10]. Recently, several novel systems have been developed to produce highly bright supramolecular fluorescence nanomaterials. One is the specialized aggregation-induced emission (AIE) and *J*-type aggregates. These fluorescence molecules do not emit in dilute solution, but they give off bright fluorescence in the condensed state. Another is dye-doped semiconducting polymer nanoparticles with high fluorescence brightness [11]. The highly fluorescent nanosized supramolecular nanoprobes/contrast agents were prepared by incorporating with functional polymer matrix, which could be further modified for targeted imaging and diagnostics. In this chapter, we will summarize recent advances in smart self-assembled nanomaterials as fluorescence probes/contrast agents for biomedical imaging, including long-term imaging, enzyme activity detection, and aggregation-induced retention (AIR) effect for diagnosis and therapy. The self-assembled nanomaterials will be classified into two groups, i.e., the ex situ and in situ self-assembled nanomaterials based on the assembly mode and the regulation strategy of fluorescence. Finally, we conclude with an outlook toward future developments of self-assembled nanomaterials for fluorescence bioimaging.

1.2 Ex-Situ Construction

1.2.1 Dye-Dispersed Nanoparticles

To prevent the ACQ effect, organic dyes can be encapsulated into polymeric matrix to form promising nanoprobes/contrast agents for bioimaging. Furthermore,

dye-dispersed nanoparticles could efficiently avoid photobleaching and produce amplified fluorescence signals due to the incorporation of several dye molecules.

Generally, hydrophobic fluorescent dyes are encapsulated within hydrophobic core of amphiphilic polymeric matrix nanoparticles (NPs) through hydrophobic interactions, which prevents the dyes aggregation and increases the stability and compatibility. The supramolecular strategies were widely used to prepare nanomaterials as nanoprobes/contrast agents for bioimaging in vitro and in vivo. Generally, the amphiphilic polymers, such as poly(acrylic acid) (PAA), [12] poly (lactic-co-glycolic acid) (PLGA), [13] and polyurethane, [14] self-assembled into nanoparticles by precipitation method with hydrophobic core and hydrophilic outer layer. The nanoparticles as nanomatrix were loaded with small-molecule fluorophores to yield dye-dispersed polymeric NPs. Compared with small fluorescence dye, dye-dispersed NPs could produce a highly amplified optical signal due to the incorporation of many dyes. However, the quantity and distribution of organic dyes in the polymeric nanomatrix are the most challenge for effectively avoiding quenching.

It is difficult to accurately control the quantification and distribution of dispersed dyes in self-assembled nanoparticles. Therefore, the highly ordered structure such as micelles [15], nanofibers [16], nanowires [17], and nanotubes [18] are constructed through defined supramolecular interactions, where small organic dyes could be well loaded and controlled with desirable aggregation level and optical properties. For example, Wang and Frank prepared NIR absorbing and emission squaraine (SQ) dyes, which have good stability and high photoresistance. They modulated the aggregation of SQ dyes in amphiphilic phospholipid bilayers of liposomes to achieve NIR fluorescence and PA tomography dual-modular imaging (Fig. 1.2) [19]. The liposomes with variable mixing ratios between SQ dyes and the liposome are typical vesicular structures with a size of 76 $\pm$ 15 nm, which is in accordance with the dynamic light scattering (DLS) result (Size: 103 $\pm$ 14 nm, PDI: 0.18). When doping minimal amounts of SQ (1:500), molecularly dispersed SQ in bilayers shows remarkable fluorescence (Fig. 1.2). Interestingly, the PA signals are enhanced with the increase of SQ dyes in the nanoconfined bilayer region, which are due to the formation of SQ-based H-aggregates and enhanced thermal conversion efficiency (Fig. 1.2). NIR fluorescence imaging in vivo indicated that the majority of SQ $\subset$ L are enriched in the area where the blood vessels are generated. The research indicated that the importance of supramolecular modulation (monomer or aggregation) of NIR dyes loaded in the nanomatrix, which will determine the characteristics and application of the dye-dispersed nanomaterials. For fluorescence bioimaging, the dyes should be well dispersed in monomer states to prevent the ACQ effect and obtain high fluorescence signals.

Besides construction of nanomatrix with highly ordered structure, doping with ionic liquid-like salts of a cationic dye with a bulky hydrophobic counterion that serves as spacer is another strategy to prevent undesirable aggregation for dye-dispersed nanoparticles. In this case, the polymeric nanoparticles can be loaded with up to 500 dyes and show higher brightness than quantum dots due to the minimization of dye aggregation and self-quenching, which also exhibit

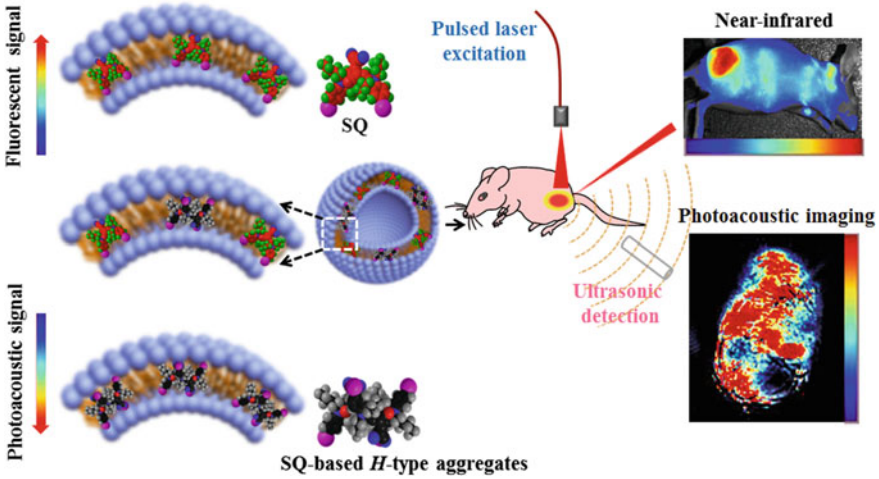

Fig. 1.2 Schematic diagram of the nanoconfined SQ assemblies in phospholipid bilayer and the utilization of these vesicles as probes for dual-modular tumor imaging in vivo. (Reproduced with permission. Copyright 2014, American Chemical Society)

photoinduced reversible on/off fluorescence switching. These dye-dispersed NPs show absence of toxicity and can be utilized for super-resolution cell imaging with high signal-to-noise ratio. Moreover, the fluorescence obtained from chemiluminescence was applied to image hydrogen peroxide, which is overexpressed under specific pathological condition. Lee et al. demonstrated that nanoparticles formulated from peroxalate esters and fluorescent dyes can image hydrogen peroxide in vivo with high specificity and sensitivity. The peroxalate nanoparticles can be loaded with fluorescence dyes, where chemiluminescent reaction between peroxalate esters and hydrogen peroxide produce light from fluorescent dyes. The emission wavelength of the peroxalate nanoparticles can be tuned by incorporating different dyes from 460 to 630 nm. Furthermore, excellent sensitivity and specificity for hydrogen peroxide over other reactive oxygen species are highly needed for in vivo imaging. The peroxalate nanoparticles are demonstrated with the capability of imaging hydrogen peroxide in the peritoneal cavity of mice during a lipopolysaccharide-induced inflammatory response.

Proteins, such as human serum albumin (HSA) and bovine serum albumin (BSA), are of the nanoscale in size with excellent biocompatibility. They can act as nanocarrier to combine with fluorescent molecules via self-assembly, forming fluorescent nanoprobes/contrast agents. HSA is a good biological nanosized carrier, which is used to self-assemble complexes with the NIR dye [20–23]. The self-assembled nanoparticles with high fluorescence quantum yield can be utilized for NIR bioimaging. On the other hand, they showed photothermal effect or photodynamic properties due to the NIR dyes, which can further show therapeutic effect for cancer and so on. BSA is another protein-based nanomatrix, which can carrier organic dyes through hydrophobic interactions to form fluorescence

nanoprobes/contrast agents [24]. SQ dyes are a kind of promising NIR fluorophores with high absorption coefficients, bright fluorescence, and photostability. Wang and Frank utilized BSA as a biocompatible carrier to obtain a highly stable supramolecular adducts of SQ and BSA (SQ ⊂ BSA) for tumor-targeted imaging and photothermal therapy in vivo (Fig. 1.3). SQ was selectively bound to BSA hydrophobic domain via hydrophobic and hydrogen-bonding interactions with up to 80-fold enhanced fluorescence intensity (Fig. 1.3a, b). By covalently conjugating target ligands to BSA, the SQ ⊂ BSA is capable of targeting tumor sites. According to the biodistribution of SQ ⊂ BSA monitored by fluorescence imaging, the photothermal therapy can be carried out effectively in vivo (Fig. 1.3d). The intrinsic chemical instability and self-aggregation properties of NIR dyes in physiological condition could be solved by protein carrier.

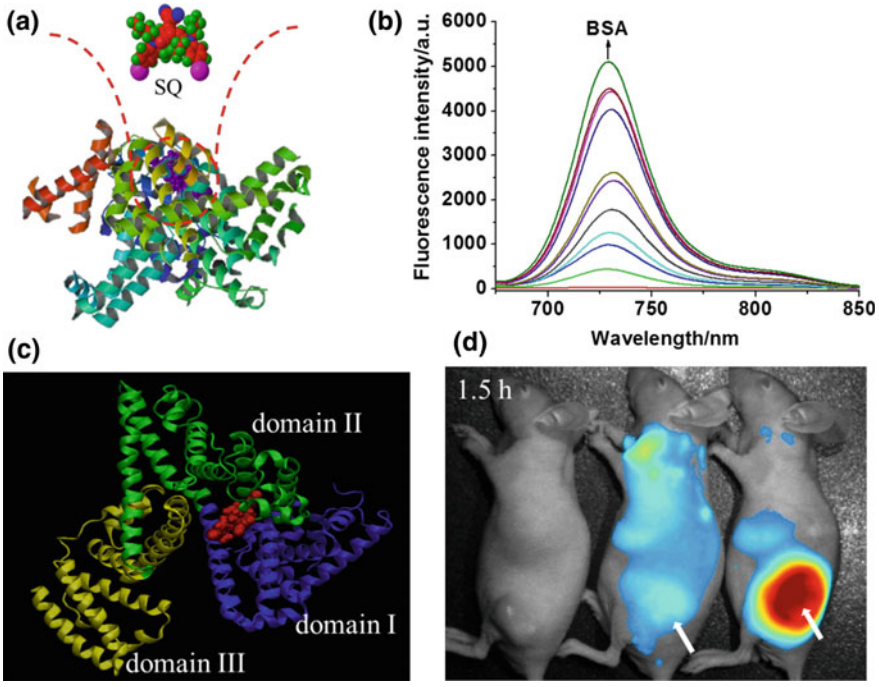

Fig. 1.3 **a** Schematic diagram of SQ dyes and BSA adducts (SQ ⊂ BSA). **b** Change in fluorescence intensity of SQ (1 μM) with the addition of BSA in phosphate buffer. The concentration of BSA was from 0, 1.1 to 12.1 μM. Excitation wavelength = 710 nm. **c** Molecular structure of site-selective binding of SQ with BSA: site I in domain II. **d** In vivo NIR optical imaging of nude mice bearing KB tumors at 1.5 after tail vein injection of the SQ ⊂ BSA and SQ ⊂ BSA-FA adducts. (The arrows show the location of subcutaneous tumors)

1.2.2 Semiconducting Polymer Nanoparticles

Semiconducting polymer nanoparticles (SPNs) emerge as a new class of promising fluorescence probes/contrast agents with excellent optical properties [25–29]. The advantages of SPNs include simple synthesis and separation procedures, excellent photostability, low cytotoxicity, high quantum yield. (Fig. 1.4) [30, 31]. The semiconducting polymer nanoparticles have been demonstrated for fluorescence, chemiluminescence, and persistent luminescence for real-time and targeted imaging in vitro and in vivo [30–32]. Generally, the SPNs are prepared by the reprecipitation method. The semiconducting polymer dissolved in a "good" solvent is rapidly added to an excess of "poor" solvent under ultrasonic dispersion. Later on, Chiu and his coworkers developed a modified method, which is called as nanoprecipitation method to obtain small and uniform SPNs with specific groups on the surface. Typically, an amphiphilic comb-like polystyrene polymer (PS-PEG-COOH)

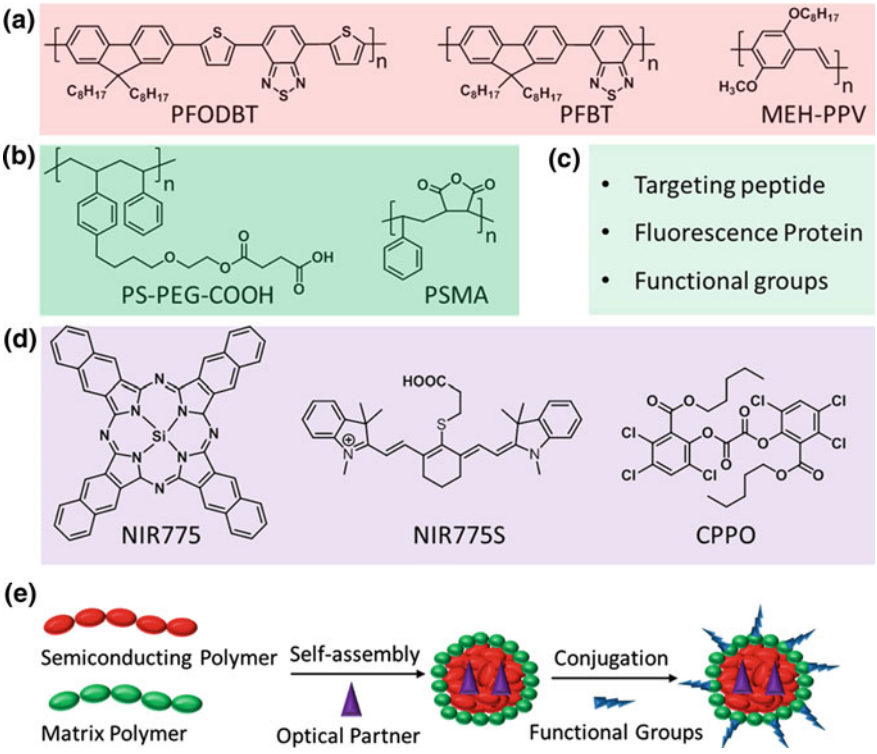

Fig. 1.4 Molecular components and preparation process of SPNs. **a** The host semiconducting polymer PFODBT, PFBT, and MEH-PPV; **b** the matrix polymer including a PEG-grafted poly (styrene) copolymer and PSMA; **c** the conjugated functional groups; **d** the optical partner, such as FRET acceptor NIR775, ROS responsive dye NIR 755S, and chemiluminescent substrate CPPO that serves as CRET energy donor; **e** the schematic illustration of preparation process of SPNs

or poly(styrene-co-maleic anhydride) (PSMA) is used to functionalize highly fluorescent SPNs (Fig. 1.4a, b) [28, 29]. Firstly, a weight ratio of 4/1 of semiconducting polymer to matrix was mixed in THF to form a homogeneous solution. Secondly, the resulting THF solution was added to two fold volume of water under ultrasonication. Finally, the organic solvent was evaporated under an inert gas atmosphere. The SPNs have an average diameter of about 15 nm and contain more than 80% of effective fluorophores. Moreover, this strategy produces surface-functionalized NPs with both PEG and carboxylic groups, which ensure good stability and high reactivity with biomolecules, such as antibodies or streptavidin. By using this strategy, they prepared highly stable SPNs, which approximately 15 times brighter than the commercial quantum dots for in vivo tumor imaging. Similarly, they attached the temperature sensitive dye Rhodamine B (RhB), whose emission intensity decreases with increasing temperature within the matrix of SPNs [26]. Accordingly, they employed SPN-RhB as a ratiometric temperature sensor for measuring intracellular temperatures in a live-cell imaging mode. The exceptional brightness of SPN-RhB allows this nanoscale temperature sensor to be used also as a fluorescent probe for cellular imaging.

Rao and his coworkers have been worked on SPNs for several years. They have demonstrated for fluorescence, chemiluminescence, and photoacoustic imaging in living cells and small animals (Fig. 1.4c–e) [11, 30–35]. They report the first example of SPNs that can emit persistent luminescence with a lifetime of nearly 1 h after a single excitation exposure to white light and show potential for in vivo optical imaging [32]. The SPNs show both NIR persistent luminescent and fluorescent emissions. The persistent luminescent emission has been applied for in vivo optical imaging in mice, which provides support for future applications in cell tracking and molecular imaging. Moreover, they introduce fluorescence resonance energy transfer (FRET) and chemiluminescence resonance energy transfer (CRET) mechanism into SPN system to detect drug-induced reactive oxygen species (ROS) and reactive nitrogen species (RNS), which can direct evaluate acute hepatotoxicity [31]. Briefly, the ROS and RNS responsive motif was loaded into the SPNs to form FRET system and CRET system with different emission wavelength, respectively. The responsive SPNs simultaneously and differentially detect RNS and ROS using two optically independent channels. They image ROS and RNS to reflect drug-induced hepatotoxicity and its remediation longitudinally in mice after systemic challenge with acetaminophen or isoniazid. Similarly, Rao and his coworkers designed self-luminescing NIR nanoparticles by integrating bioluminescence resonance energy transfer (BRET) and FRET mechanism [30]. The NIR SPNs were prepared by nanoprecipitation using poly[2-methoxy-5-((2-ethylhexyl) oxy)-p-phenylenevinylene] (MEH-PPV, FRET donor) and NIR775 (FRET acceptor) as the emitters and PS-PEG-COOH as the matrix, followed by conjugation with a bioluminescent eight-mutation variant of luciferase (Luc8) and RGD peptide. Three emission peaks from MEH-PPV, Luc8, and NIR775 are located at 480, 594, and 778 nm, respectively, indicating efficient BRET from Luc8 to MEH-PPV, followed by FRET from MEH-PPV to NIR775. Upon intravenous administration of the SNPs into mice, strong NIR fluorescence signals were observed from the

lymphatic networks, including neck lymph nodes, axillary lymph nodes, inguinal lymph nodes, and lateral thoracic lymph nodes. The self-luminescing feature provided excellent tumor-to-background ratio for imaging very small tumors (2–3 mm in diameter). The novel self-luminescing nanoparticles provided highly improved sensitivity through bioluminescence imaging in in vivo studies, such as lymph-node mapping and cancer imaging.

The SPNs were prepared through microemulsion method with, poly (DL-lactide-co-glycolide) (PLGA) as matrix polymer, which is a Food and Drug Administration approved biocompatible polymer [36]. The PLGA-encapsulated SPNs (240–270 nm) have the terminal carboxyl groups of PLGA, which can be further conjugated with functional groups before or after SPN formation. Meanwhile, Liu and coworkers developed a general strategy through a single emulsion method to fabricate a series of SPNs with PLGA as nanomatrix, which showed emission in the range of 400–700 nm [37]. The quantum yields of the SPNs were 4–25 folds lower than those of semiconducting polymer in THF solutions, due to extensive semiconducting polymer aggregation in nanoparticles. Liu et al. introduced bulky groups (POSS) to poly(fluorenevinylene) to prevent close-packing of semiconducting polymer inside the SPNs. The reformative poly(fluorenevinylene) and PLGA-based SPNs showed an improved quantum yield of 19% relative to 11% for poly(fluorenevinylene) [38]. The surface carboxyl groups of PLGA nanoparticles were further modified with trastuzumab through coupling reaction. The trastuzumab-functionalized SPNs were then successfully used for specific discrimination of SK-BR-3 cells from MCF-7 and NIH/3T3 cells.

1.2.3 AIE Nanoparticles

Aggregation-induced emission (AIE) and aggregation-induced emission enhancement (AIEE) mechanism have been developed by Tang, which can obtain high fluorescence in aggregated state (Fig. 1.5a) [8, 39–47]. Tang and his coworkers discovered that AIE was exactly opposite to ACQ effect (Fig. 1.5b). The typical AIE fluorogenic molecules are nonemissive when molecularly dissolved but highly emissive when aggregated due to the restriction of intramolecular rotations (RIR). The AIE phenomenon is generally observed in molecules with rotating units such as phenyl rings. In dilute solutions, the rotor-containing fluorogens undergo low-frequency motions, resulting in fast nonradiative decay of the excited states and nonemissive of fluorogens. In the aggregates, the intermolecular steric interaction blocked the intramolecular rotations, leading to the emission of fluorogens when absorbed energy. The AIE effect made the fluorogens ideal candidate materials for the preparation of fluorescent nanoparticles with highly emissive fluorescent signals. In recent years, a large variety of AIE molecules have been developed, which have propeller-shaped structures and freely rotatable peripheral aromatic moieties. A few typical examples such as tetraphenylethene (TPE), hexaphenylsilole (HPS),

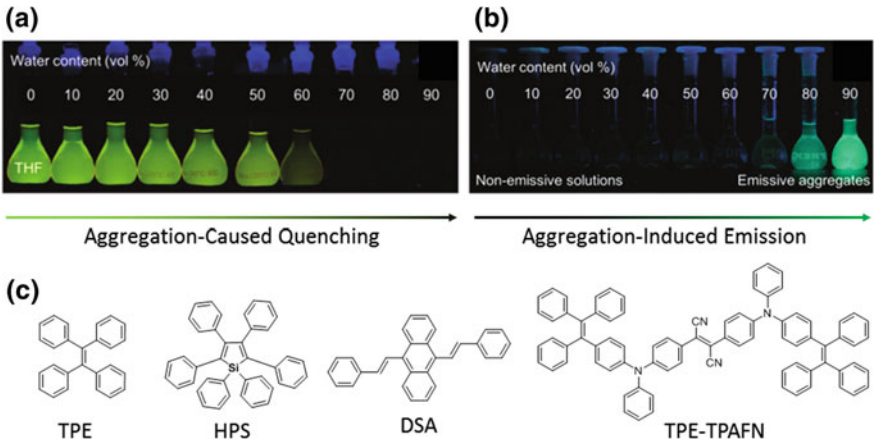

Fig. 1.5 **a** N,N-dicyclohexyl-1,7-dibromo-3,4,9,10-perylenetetracarboxylic diimide (DDPD) and **b** HPS in THF–water mixtures with different water contents for fluorescence photographs of solutions/suspensions. **c** Typical AIE luminogens TPE, HPS, DSA, TPE-TPAFN. (Reproduced with permission [39]. Copyright 2011, the Royal Society of Chemistry)

distyreneanthracene (DSA), and TPE conjugated 2,3-bis-[4-(diphenylamino)phenyl] fumaronitrile (TPE-TPAFN) are shown in Fig. 1.5c.

The AIE nanoparticles showed high stability and strong retention in living cells, which could be utilized for long-term cell imaging for many passages. For example, the aminated HPS derivatives spontaneously aggregated into $\sim$220 nm nanoparticles in aqueous media [48]. The nanoparticles effectively stained HeLa cells with bright green fluorescence and enabled long-term cell tracing up to four passages. Furthermore, the TPE based AIE nanoparticles may allow cell tracing for 10–15 passages [49, 50]. The strong retention of the AIE nanoparticles with high concentrations enabled visual monitoring of the cell growth, which was better than the commercial cell tracker.

BSA and functionalized BSA were also utilized to encapsulate an AIE molecule for bioimaging [51, 52]. For example, attaching of two TPE units with 2-2,6-bis [(E)-4-(diphenylamino)styryl]-4H-pyran-4-ylidene-malononitrile can afford an AIE molecule (TPE-TPA-DCM), which was imparted AIE characteristics by conjugation of AIE active TPE. The TPA-DCM in THF was added to BSA aqueous solution under sonication followed by crosslinking with glutaraldehyde, forming TPE-TPA-DCM-loaded BSA nanoparticles with bright fluorescence [51]. The TPE-TPA-DCM BSA nanoparticles can enter MCF-7 cells and accumulate in tumor for in vitro and in vivo imaging. Furthermore, the BSA was functionalized with arginine–glycine–aspartic acid (RGD) peptide to yield fluorescent probes for specific recognition of integrin receptor-overexpressed cancer cells.

Besides traditional conjugation of the targeting groups with AIE molecules to afford specific cell imaging, the functionalized AIE nanoparticles could be prepared by a precipitation strategy. The AIE molecules were encapsulated and stabilized

with 1,2-distearoyl-sn-glycero-3-phosphoethanolamine-N-[methoxy (polyethylene glycol)] (DSPE-PEG) [53]. The functional groups such as targeting molecules and peptides can be introduced by co-assembly with pre-conjugated DSPE-PEG. The typical preparation process was shown in Fig. 1.6. THF solution of AIE molecule, DSPE-PEG_{2000}, and DSPE-PEG_{5000}-folate was added into water under continuous sonication, resulting in 90 nm AIE nanoparticles with fine-tuned surface folic acid density. The AIE nanoparticles could selectivity recognize MCF-7 from NIH3T3 cells due to the specific folate receptor-mediated endocytosis for MCF-7 cells. The supramolecular strategy showed many advantages including convenient preparation and well-controlled density of functional group on the surfaces.

The active DSPE-PEG_{2000}-R (R = NH_2, COOH, N-maleimide) could be also involved in the precipitation strategy to prepare AIE nanoparticles with surface functional groups [54–56]. As a result, the AIE nanoparticles could be post-modified with functional peptides, proteins and so on, which was much easier

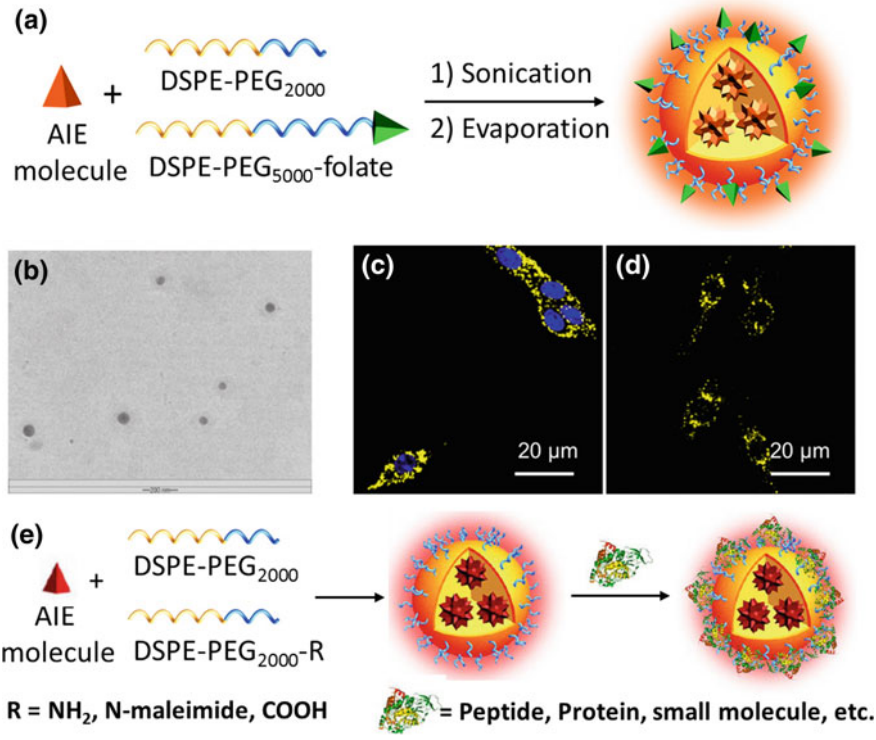

Fig. 1.6 **a** Schematic illustration of AIE nanoparticles preparation with DSPE-PEG as encapsulation matrix and the HR-TEM image (**b**). **c** One- and **d** two-photon confocal images of MCF-7 breast cancer cells after incubation with the nanoparticles. **e** Schematic illustration of the AIE-doped DSPE-PEG with post-modification. **a–d** were reproduced with permission from Ref [53]. Copyright 2011 Royal Society of Chemistry. **e** was reproduced with permission from Ref [8], Copyright 2013 American Society of Chemistry

than chemical modification of AIE molecule itself. For instance, DSPE-PEG_{2000} and DSPE-PEG_{2000}-NH_2 were used to co-assemble with AIE molecules TPE-TPAFN. TPE-TPAFN-based AIE nanoparticles showed a uniform hydrodynamic size of 30 nm with NIR emission (maximum emission: 671 nm). AIE nanoparticles were conjugated with HIV-1 transactivator of transcription (Tat) via carbodiimide-mediated coupling (Fig. 1.6e) affords TPE-TPAFN-based DSPE-PEG-Tat nanoparticles. The Tat-AIE nanoparticles show higher stability and brightness than the commercial Qtracker® 655 and realize long-term noninvasive cell tracing. The Tat-AIE nanoparticles were capable of tracing MCF-7 cells for 10–12 generations in vitro. Moreover, in vivo fluorescence imaging through monitoring AIE nanoparticle-labeled C6 glioma cells in mouse indicated that the Tat-AIE nanoparticles had the ability to trace cell at long-term up to 21 days.

Near-infrared (NIR) AIE nanoparticles were highly desirable for bioimaging, especially for in vivo application as shown in the above examples, which display nearly no spectral overlap with biosubstrate autofluorescence. In another case, the shape-tailored organic quinoline–malononitrile (QM) with AIE characteristics is designed and synthesized to form AIE nanoprobes with far-red and NIR fluorescence and well-controlled morphology (from rod-like to spherical) [57]. The QM-based AIE nanoprobes are biocompatible and highly desirable for cell-tracking applications. The tumor-targeted bioimaging performance is related to the shape of QM nanoaggregates, where the spherical shape of QM nanoaggregates exhibits excellent tumor-targeted bioimaging in vivo. Similarly, diketo-pyrrolo-pyrrole (DPP) compounds with AIE properties are NIR emissive, which is stabilized with DSPE-PEG-Mal to form AIE nanoparticles. The surface of DPP-based AIE nanoparticles is further modified with cell penetrating peptide (CPP) to yield DPP-CPP nanoparticles with high brightness, good water dispersibility, and excellent biocompatibility for cell imaging [56].

Besides the NIR fluorescence imaging, the two-photon fluorescence imaging was developed for high-resolution imaging in vivo [58, 59]. Liu et al. reported the synthesis of ultrabright 4,7-bis[4-(1,2,2-triphenylvinyl)phenyl]benzo-2,1,3-thiadiazole (BTPEBT)-based supramolecular AIE nanoparticles with small size (≈33 nm), which showed a high two-photon absorption cross section, superb colloidal stability, excellent photostability, low in vivo toxicity and used for real-time intravital two-photon imaging of blood vessels [60]. The supramolecular AIE nanoparticles were brighter than widely used organic dyes such as Evans blue for two-photon blood vessels labeling agent. Furthermore, the supramolecular AIE nanoparticles can be used to visualize the major blood vessels as well as the smaller capillaries in the pia matter with a depth of beyond 400 μm.

1.2.4 J-Aggregates

J-type aggregates of fluorophores are another straightforward solution for ACQ effect. According to the supramolecular interactions, the H- and J-aggregates were

developed with organic dyes. Based on the theoretical calculation and experimental results, H-aggregates showed blue-shifted absorption and quenched fluorescence due to the face-to-face dipole moments. However, the J-aggregates showed strong fluorescence with red-shifted absorption. Frank and Wang have been devoted to design supramolecular fluorescence based on perylenes by tuning the hydrogen bonds [61, 62]. Recently, Wang et al. designed and developed a new series of bis (pyrene) derivatives, i.e., BP1–BP4 with 1,3-dicarbonyl, pyridine-2,6-dicarbonyl, oxaloyl and benzene- 1,4-dicarbonyl as linkers, respectively (Fig. 1.7a) [63]. In solution, all compounds showed low fluorescence quantum yields ($\Phi < 1.7\%$) in variable organic solvents due to the twisted intramolecular charge transfer (TICT). In a sharp contrast, BP1 in the solid state was self-assembled to form J-type aggregates with almost 30-fold fluorescence enhancement (Φ was up to 32.6%) compared to that in solution (Fig. 1.7b, c). Nevertheless, H-type aggregates of BP3 and BP4 were observed with poor emissive efficiencies ($\Phi < 3.1\%$). Furthermore, the morphologies of supramolecular aggregates showed that BP1 and BP2 were dot-shaped nanoaggregates with 2–6 nm in diameters (Fig. 1.7d), while BP3 and BP4 showed sheet-like morphologies with 5–10 nm in width and 20–100 nm in length. The nanoaggregates of BP1 and BP2 coated with F108 surfactants showed good pH and photostability in physiological condition. Finally, the nanoaggregates of BP1 and BP2 were successfully employed as fluorescence nanoprobes for lysosome-targeted imaging in living cells with negligible cytotoxicity. To expand the application of BP derivatives, the functionalization of BP is achieved by introducing the active groups, such as COOH, NH_2, Br, N_3 (Fig. 1.7e).

To obtain the NIR emission under NIR two-photon irradiation, the BP1 was co-assembled with Nile red to form FRET two-photon fluorescence imaging

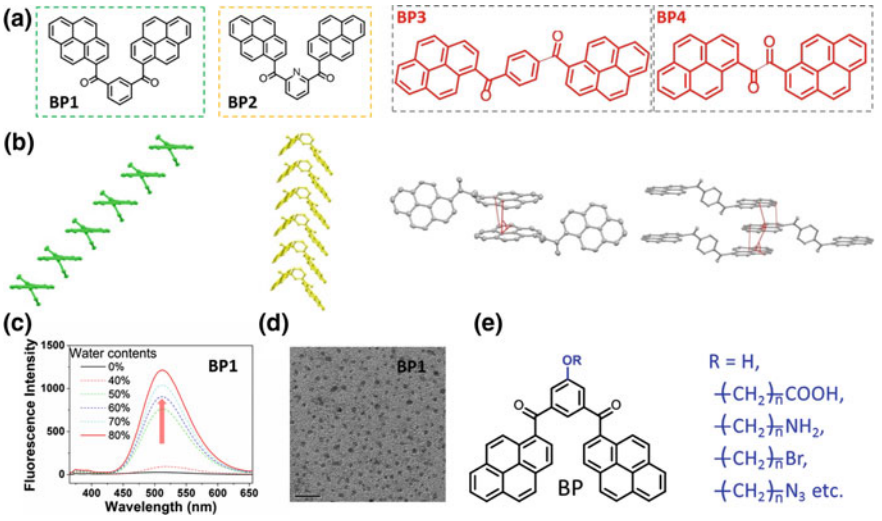

Fig. 1.7 **a** Molecular structures of bis-pyrene derivatives BP1-4 and **b** their supramolecular packing structures. **c** Typical fluorescence spectra of BP1 upon aggregation and **d** the resulting TEM image. **e** Molecular structures of functionalized BP derivatives

contrast agents, which exhibited unprecedentedly high tissue penetration capability (Fig. 1.8) [64]. The BP-NR showed a large δ (2.4×10^5 GM) value, a NIR emission (630 nm), and a high energy transfer efficiency (60.7%). The δ value of this co-assembled BP-NR nanoparticle is the highest one among all the reported two-photon contrast agent materials. The BP-NR showed deep tissue penetration up to 2200 μm in-depth in mock tissue. Finally, the low-concentrated BP-NR (0.5 nM) was successfully applied to visualize the fine structures of aligned cartilage in the ear of mice in vivo.

Other typical fluorescence molecular probes can form J-aggregates after modification with π-conjugated groups due to tailored π−π stacking. For example, a series of lipidic boron-dipyrromethene (BODIPY) dyes were designed and synthesized to self-assemble into J-aggregates with NIR fluorescence [65]. The supramolecular J-type aggregates could act as imaging probes or delivery vehicles for living cells, where the entering of J-type aggregates could be monitored directly with fluorescence microscopy. Similarly, a CF_3-linked BODIPY derivative can form strongly luminescent J-aggregates, which is in contrast with the quenched condensed-phase photophysics that are typical for BODIPY dyes. The J-aggregates show narrow red-shifted absorption and emission bands, minimal Stokes shift, and increased fluorescence rate constants. However, with the preparation of J-aggregates, the biological imaging application should be further developed [66]. In another case, 1,4-dimethoxy-2,5-di [4-(cyano)styryl]benzene (COPV) can form water-miscible J-aggregate nanoassemblies driven by the cooperation between π−π

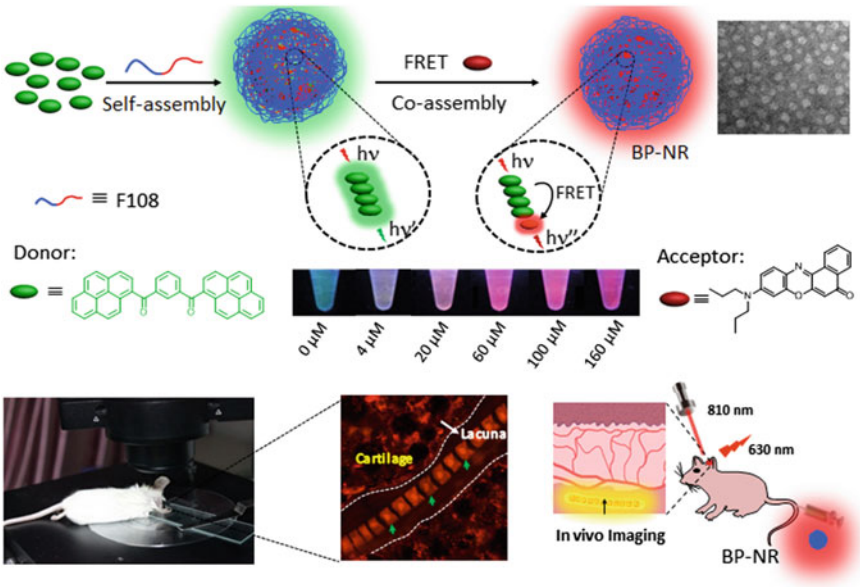

Fig. 1.8 Schematic illustration and corresponding experimental results of construction of FRET BP1-NR nanosystem and their applications for in vivo imaging

stacking and hydrogen-bonding interactions [67]. The J-aggregates based on COPV were highly emissive in aqueous media, which were also used as efficient two-photon fluorescent contrast agents for bioimaging.

1.2.5 In situ Construction

Nature can modulate the biological processes in spatiotemporal way, which involves the direct manipulation of a material, especially a supramolecular material by a stimulus over multiple length and time scales. Inspired by nature, in situ construction/reconstruction of nanomaterials strategy in biological conditions is developed to execute diagnostics and/or therapeutics with signal transmutation to solve unpredictable changes (instability) of the supramolecular nanomaterials under complicated and multivariate physiological environments when applied in vitro and in vivo. Some specific binding interactions, biocompatible reactions and pH, enzyme under specific biological conditions were applied to induce supramolecular interaction changes, such as hydrophobic interactions, resulting in in situ assembly and signal enhancement. The in situ construction was categorized as disassembly, assembly, and reassembly.

1.2.5.1 Disassembly

It is well known that fluorescence would be quenched when aggregates for most fluorescence dyes. As a result, the disassembly of fluorescence dyes is a turn-on strategy, which could be utilized for bioimaging and diagnostics (Fig. 1.9). Hamachi developed protein–ligand interactions regulated disassembly to achieve protein recognition with accompanied fluorescence signal changes [68–70]. Tumor-specific or tissue-selective protein biomarkers overexpressed on cell surfaces are important targets for basic biological research and therapeutic applications. The identification of these proteins offers direct applications in environmental monitoring and therapeutics. They carried out specific protein detection by using self-assembled fluorescent nanoprobes consisting of a hydrophilic protein ligand and a hydrophobic BODIPY fluorophore (1–5 $\sim$ 1–11) [71].

Wang and Chen et al. reported a co-assembled nanovesicle of two BODIPY amphiphiles with distinct emission color. The fluorescence of both BODIPY dyes is completely quenched and recovered upon disassembly driven by solvent variation or cell uptake. Accordingly, the co-assembled nanoaggregates were demonstrated for dual-color imaging of live cells. Furthermore, dual-color and ratiometric fluorescence imaging of live cells indicated that the disaggregated dyes are localized on the endoplasmic reticulum [72]. In the same group, Wang and Qiao et al. demonstrated BP disassembly modulated by a pH-sensitive polymer nanocarrier [73]. The BP was conjugated with hydrophilic poly(amino ester)s (as a pH-sensitive carrier, P-BP). The P-BP could self-assemble into nanoparticles through

1-	1	2	3	4	5	6	7	8	9	10	11
R_1	3	3	4	2	1	1	1	1	1	3	3
R_2	-	-	-	-	-	-	1	2	5	3	4
R_3	1	3	1	1	1	2	2	2	3	2	2
Linker	2	2	3	3	1	3	3	3	3	3	3
x	5	5	10	10	10	10	10	10	10	10	10
m	-	-	5	5	5	5	5	5	5	5	5
n	1	1	-	-	-	-	-	-	-	-	-

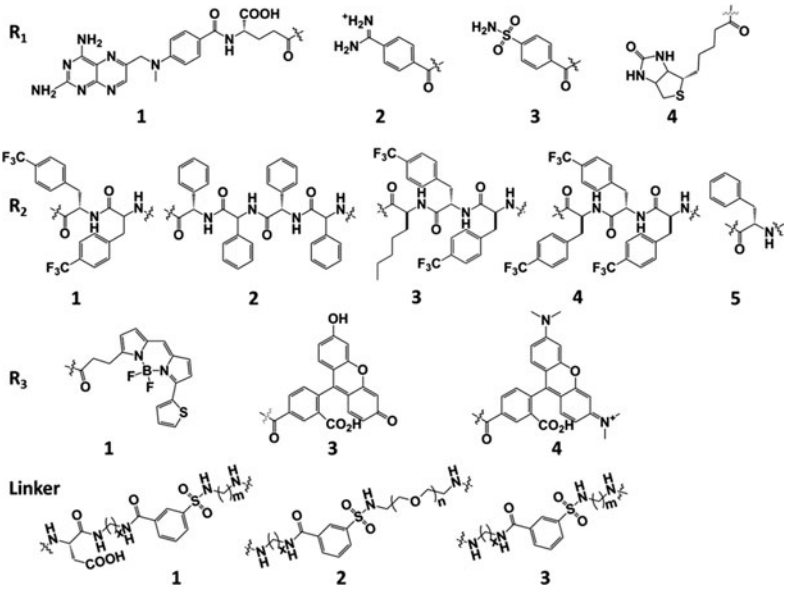

◂**Fig. 1.9** Protein detection developed by I. Hamachi, the fluorescence probe quenched when self-assembled in aqueous solution. The fluorescence on after disassembled due to the protein recognition

hydrophobic interactions at neutral pH, where the BP aggregated as the hydrophobic core with green fluorescence and polymer as the hydrophilic shell. As the pH decreased, the protonation of polymer chains induced the swelling of nanoparticles with disaggregation of BP. As a result, blue fluorescence of BP monomer increased with decrease of green fluorescence from BP aggregates due to the disassembly. The disassemble nanoparticles could in situ monitor pH values in living cells.

Through protein binding, the supramolecular self-assemblies could be disassembly for sensing, drug delivery, and diagnostics. The structural and functional aspects of assemblies formed from amphiphilic dendrimers can show reversible assembly/disassembly depending on the nature of the solvent medium [74–76]. S. Thayumanavan introduces a new approach of protein-responsive supramolecular disassembly for detection or specific-responsive release of drugs. The amphiphilic dendrimers self-assembled into nanomicelle with hydrophobic guest molecules in their interiors, the stability of which is dependent on the relative compatibility of the hydrophilic and hydrophobic functionalities with water, often referred to as hydrophilic–lipophilic balance (HLB). The protein binds the ligands on amphiphilic dendrimers and induces the changes of HLB, resulting in the disassembly and drug release. In another example, a detection method for specific protein is achieved by using this method. The ligand-tethered fluorophore/quencher pairs are encapsulated in the micellar assemblies through noncovalent interactions, where the fluorescence is in the "off" state. Protein-binding-induced dissociation of the ligand-fluorophore combination away from micelles turns the fluorescence to the "on" state. Based on the fluorescence signals, the protein can be recognized and detected. The detection of protein can provide a unique opportunity to explore imbalances in protein activity, which are the primary reasons for most human pathology [76].

1.2.5.2 Assembly

The in situ self-assembly is generally realized from the small molecule with hydrophobic aggregatable units and hydrophilic responsive groups (prevent the aggregation due to hydrophilicity and steric hindrance). The hydrophobic aggregatable units self-assemble when the hydrophilic group left upon physiological condition stimuli. The strategy was proposed by Xu and his coworkers, who are experts on hydrogel and developed supramolecular hydrogelation inside living cells in situ [77]. They prepared a precursor of fluorescent hydrogelator, which consists of a fluorophore, 4-nitro-2,1,3-benzoxadiazole (NBD), and a phosphorous ester on the tyrosine residue of a small peptide. The NBD group is a fluorophore known to give more intense fluorescence in hydrophobic environment than in water. The

alkaline phosphatase (ALP) catalyzed dephosphorylation can afford a more hydrophobic hydrogelator than the precursor, which is able to self-assemble in water to form nanofibers and to result in the hydrogel. Therefore, the individual hydrogelators exhibit low fluorescence, and the nanofibers of the hydrogelators display bright fluorescence. On the one hand, the strategy allowed the evaluation of intracellular self-assembly, the dynamics, and the localization of the nanofibers of the hydrogelators in live cells. On the other hand, the in situ self-assembly with enhanced fluorescence showed its potential for wash-free cell imaging method. This approach explores supramolecular chemistry inside cells and may lead to new insights, processes, or materials at the interface of chemistry and biology [78].

Rao and Liang reported a condensation reaction-induced hydrophobicity increase, resulting in aggregation to form nanostructures. The condensation reaction can be controlled by reduction or enzyme under physiological conditions with fluorescence readout. The typical condensation reaction could be accomplished between 1,2-aminothiol and 2-cyanobenzothiazole in vitro and in living cells under the control of either pH, disulfide reduction, or enzymatic cleavage [79–82]. The self-assembled nanostructures of the condensation products were fully characterized, which could be controlled by tuning the structure of the monomers. By applying this condensation reaction-induced assembly, they monitored the caspase-3/7 activity in vitro and in vivo with fluorescence imaging technique [81]. The fluorescent small molecule Cy5.5 was introduced into condensation reaction system, and self-assembled with the condensation reaction to with the enhanced fluorescence. The caspase-3/7 activities were imaged successfully in both apoptotic cells and tumor tissues using three-dimensional structured illumination microscopy.

Tang et al. developed the AIE NPs for fluorescence bioimaging; furthermore, they constructed AIE-based supramolecular aggregates in living cells, where the AIE molecules were released from their conjunction with peptide. They combined DEVD peptide and TPE modules to image the caspase-3 activity [83]. Later on, they extended the AIE detection system by combining the chemotherapeutic drug and biological evaluated chemotherapeutic effect [84]. They synthesized a functionalized Pt(IV) prodrug with a cyclic arginine–glycine–aspartic acid (cRGD) tripeptide for targeting integrin $\alpha_v\beta_3$ overexpressed cancer cells and an apoptosis sensor which is composed of TPS fluorophore with AIE characteristics and a caspase-3 enzyme specific Asp-Glu-Val-Asp (DEVD) peptide. The Pt(IV) prodrug can be selectively and effectively uptaken by $\alpha_v\beta_3$ integrin overexpressed cancer cells. Then, the Pt(IV) prodrug can be reduced to produce active Pt(II) drug and release the apoptosis sensor TPS-DEVD simultaneously in cells. The cell apoptosis can be induced by Pt(II) drug and detected by DEVD-TPS, which is cleaved by caspase-3 enzyme and aggregated with fluorescence enhancement. Such noninvasive and real-time imaging of drug-induced apoptosis in situ can be used as an indicator for early evaluation of the therapeutic responses of a specific anticancer drug. The other enzymes such as cathepsin B [85, 86] and alkaline phosphatase [87] are also used to trigger the aggregation of AIE molecule for in situ imaging.

In the Wang group, the bis-pyrene was developed for J-type aggregate with strong emission in water. They reported supramolecular approach to realize the

in situ formation of nanoassemblies in living cells, which involved the pH-responsive amphiphilic carrier and aggregatable monomer BP [88]. The nanocarrier delivered the BP to the lysosomes of cells. In the acidic lysosomes, the bis-pyrene monomers were released and self-aggregated with turn-on fluorescence. The bis(pyrene) derivatives (BP, aggregatable monomer) were molecularly dispersed in the hydrophobic domains of pH-responsive amphiphilic poly(β-amino esters) (PbAE) micelles (responsive carrier) at pH 7.4 via hydrophobic interactions. BP was released and self-aggregated with significant fluorescence enhancement due to the formation of aggregates at pH 5.5 in phosphate buffered solution or serum free cell culture medium (opti-MEM). The release and aggregation of BPs with 6-fold fluorescence enhancement were accomplished within 15 s at 15 μM. Based on unique properties of the supramolecular system, the in situ self-aggregation process of BPs with turn-on fluorescence was successfully achieved in living cells. First, BPs dispersed micelles were accumulated in the lysosomes. Then, the BPs were released and self-aggregated with turn-on fluorescence upon the formation of nanoaggregates in acidic lysosomes. They have demonstrated a supramolecular system to achieve in situ self-aggregation in living cells. The BPs could be transferred into the lysosomes of living cells by dispersing into pH-responsive PbAE micelles via endocytosis. In acidic environment of the lysosomes, the BPs were released and self-aggregated in situ, which was validated by turn-on fluorescence and TEM images of BPs nanoaggregates inside Hela cells. This designed supramolecular strategy is a versatile platform for incorporation of aggregatable monomers into cellular environment-responsive carrier modules, leading to in situ self-aggregation in living objects, which will open a new avenue for highly sensitive molecular diagnostics in the future.

In the same group, they utilized an enzymatic method to modulate the BP aggregates in the living cells to achieve the real-time monitoring autophagy [89]. The intelligent building blocks (DPBP) were composed by a bulky dendrimer carrier, a bis(pyrene) derivatives (BP) as a signal molecule, and a peptide as a responsive unit that can be cleaved by an autophagy-specific enzyme, i.e., ATG4. DPBP maintains the quenched fluorescence in monomer state. However, the responsive peptide is specifically tailored upon activation of autophagy, resulting in self-aggregation of BP residues and 30-fold enhanced fluorescence. By measuring the fluorescent signal values, the autophagic level could be quantitatively evaluated.

1.2.5.3 Reassembly

Molecular self-assembly plays an important role in construction of a variety of functional high-ordered nanostructures with precise arrangements in biological systems [90, 91]. The well-defined structure and morphology impart the feature functionality to self-assemblies. Interestingly, smart self-assemblies formed by peptide-based building blocks showed morphology transformation upon stimuli such as enzyme, [92, 93] pH, [94] photoirradiation [95, 96]. The advantages of each morphology can be realized by in situ transformation in vivo for high-performance

biological applications. For examples, drug release during the transformation with good controllability in certain time can enhance pharmacology and drug efficacy; [94, 97] the nanoparticles would show prolonged retention effect when they were precisely controlled in transformation into nanofibers [93].

For instance, Giannechi reported the enzyme-responsive spherical nanoparticles form an aggregate-like scaffold or micrometer scale assemblies when activated by metalloproteinase. They utilized enzyme-responsive material to present an in situ reassembly of nanoparticles [92]. First, they described an enzyme-programmed tissue-targeted nanoparticle probe and utilized a Förster resonance energy transfer (FRET)-based assay for monitoring particle accumulation. Generation of a FRET signal provided evidence that the nanoparticles had undergone an enzyme directed aggregation process in tumor tissue generating a slow clearing, self-assembled "implant" of polymeric material within the tissue. Later on, they have utilized Alexa Fluor 647-conjugated peptide polymeric nanoparticles as probes for whole mouse imaging and show extended tumor retention via morphological aggregation in response to MMP enzyme cleavage. Furthermore, they provided compelling evidence that this accumulation process is due to assembly of nanometer particles into larger-scale aggregates by employing super-resolution fluorescence microscopy (stochastic optical reconstruction microscopy, STORM) to study tumor tissue slices ex vivo. They observed fluorescent aggregates in targeted tumor tissues within 1 h that were retained for at least 1 week via detailed tissue-slice analysis coupled with whole animal NIR-fluorescence imaging. Most importantly, particles designed to resist reaction with MMPs were cleared from tumor tissues within 1 h as observed in both in vivo and ex vivo STORM and confocal fluorescence analysis of tissue slices. They validated that the materials had passively diffused into the tumors following injection and then undergone further aggregation with a size increase, which trapped the material within the extracellular space within the tissue.

At the same time, they utilized the same strategy to target the myocardial infarction (MI) as well for achieving prolonged retention of a material in an acute MI via intravenous injection [93]. The nanoparticles were designed to respond to enzymatic stimuli matrix metalloproteinases (MMPs) present in the acute MI resulting in a morphological transition from discrete micellar nanoparticles into network-like scaffolds. The fluorescent nanoparticle is composed of brush peptide–polymer amphiphiles (PPAs) based on a polynorbornene backbone with peptide sequences specific for recognition of MMP-2 and MMP-9. IV delivery allows the enzyme-responsive nanoparticles to freely circulate in the bloodstream until reaching the infarct through the leaky post-MI vasculature, where they assemble and remain within the injured site for up to 28 d post-injection. For the MI application described here, the polymer design was modified to optimize net polymer amphiphilicity. They reduced the degree of polymerization of the hydrophilic block and degree of conjugation of hydrophilic peptide such that the hydrophilic weight fraction was 0.45 instead of 0.55, which increased the responsiveness of the system by decreasing the peptide brush density within formulated micelles of the same size. The in situ assembly in targeted tissue provided a promising approach for long-term imaging and sustained delivery of therapeutics.

Stupp's group prepared pH-responsive peptide amphiphiles, which self-assembled into nanofibers at pH of 7.5 and transformed into nanoparticles with the decreasing pH [94]. By incorporating an oligo-histidine H_6 sequence with aliphatic tail on the N-terminus or near the C-terminus, they developed two peptide amphiphiles that self-assembled into distinct morphologies on the nanoscale, either as nanofibers or spherical micelles. Upon protonation of the histidine residues in acidic solutions (pH 6.0 and 6.5), the nanofibers of peptide amphiphiles could transform into nanoparticles at pH 6.0. Meanwhile, the sphere-forming peptide amphiphiles disassembled with impaired hydrogen-bonds. Interestingly, the H_6-based nanofiber assemblies encapsulated camptothecin (CPT) with up to 60% efficiency, a sevenfold increase in CPT encapsulation relative to spherical micelles. The peptide amphiphiles were labeled with AF680 to image the biodistribution to understand the effect of shape and pH-dependent assemblies on tumor accumulation in vivo. The results indicated the high accumulation of peptide amphiphiles in mammary tumor as determined by tumor fluorescence. Additionally, pH-sensitive nanofibers showed improved tumor accumulation over both spherical micelles and nanofibers that did not change morphologies in acidic environments. The study demonstrated that the morphological transitions upon changes in pH of supramolecular nanostructures affect drug encapsulation and tumor accumulation.

Wang et al. reported a glutathione (GSH)-based bio-orthogonal reaction that triggers reconstruction of self-assembled nanostructures, resulting in turn-on of dual-color fluorescence signals in living cells [98]. They prepared a cyanine-based amphiphilic dye (BP-S-Cy) with a bis(pyrene) substitution. The BP-S-Cy was initially self-assembled into nanoparticles with quenched fluorescence in water. Second, upon BP-S-Cy was selectively cleaved and substituted by GSH, the released hydrophobic BP unit self-assembled into larger nanoaggregates with almost 36-fold fluorescence enhancement with emission maxima at 520 nm. Meanwhile, the newly formed GSH labeled Cy (Cy-GSH) exhibited 30-fold fluorescence enhancement at NIR region (λ_{em} 820 nm). Finally, this new GSH triggered bio-orthogonal reaction and resultant reconstruction of self-assembled nanostructures were validated in living cells. This smart nanoprobe was utilized to image the GSH in living cells with dual-wavelength emission.

The understanding of formation and structure-evolutionary mechanism of self-assembled superstructures is still a challenge. Wang and his coworkers designed and prepared a series of supramolecular building blocks (BP-KLVFFG-PEG, BKP) composed by an aromatic bis-pyrene motif, a hydrogen-bonding motif, and a hydrophilic poly ethylene glycol (PEG) chain and investigated their self-assembly processes systematically (Fig. 1.10) [99]. BP was chosen as hydrophobic core to induce aggregation and monitor the aggregation by fluorescence signals from BP upon aggregation. The peptide with a sequence of Lys-Leu-Val-Phe-Phe (KLVFF) originated from the segments of amyloid β has been proven to be a highly fibrillation by H-bonds [100]. The polymeric peptide (KLVFF) was chosen as peptide scaffolds for inducing fiber formation. It is well known that hydrophilic–lipophilic balance (HLB) affects the self-assembly process, and resultant structures and morphologies of supramolecular nanomaterials [101].

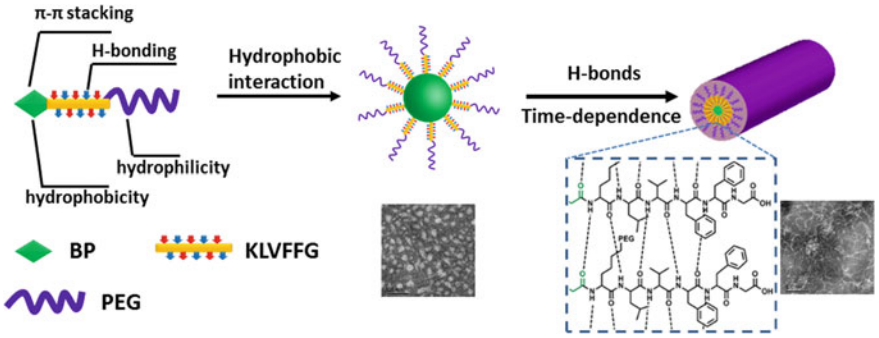

Fig. 1.10 Schematic illustration of In situ formation of nanofibers from nanoparticles of BP-KLVFFG-PEG polymer peptide and corresponding TEM images

The PEG with different molecular weights (Mw = 368, 1000, 2000) was chosen as hydrophilic chains to modulate HLB of the target molecules. The study revealed that the hydrophobic and π−π interactions initially drove the self-assembly of BKP into nanoparticles with *J*-type fashion, and the H-bonding interactions further drove in situ spontaneous morphology transformation into nanofibers. The longer was hydrophilic chain, the faster transformation was from nanoparticles to nanofibers. The elucidation of BKP assemblies from the molecular level to supramolecular nanosystems constitutes a bridge between molecular structures and their morphologies.

Based on the above systematical investigation of morphology transformation, the metal ions-regulated morphology transformation was proposed and confirmed in the same group [102]. It is well known that RGD has specific binding activity to integrin $\alpha_v\beta_3$, which is mainly driven by the coordination interactions between RGD and the metal ions (Ca^{2+}, Mg^{2+}) at "metal ion-dependent adhesion site" (MIDAS) [103–105]. They designed and prepared modular peptide-based building blocks (BKR) composed by an aromatic bis-pyrene (BP) motif, a Lys-Leu-Val-Phe-Phe (KLVFF) motif, and a divalent cation (Ca^{2+}) binding motif (Arg-Gly-Asp, RGD). The study demonstrated metal ion-mediated structural evolution of peptide-based superstructures on specific cancer cell surfaces for interfering cellular viability by applying the RGD and integrin $\alpha_v\beta_3$ interactions. Actually, the BKR could light up calcium alginate beads and U87 cells through binding with the Ca^{2+} on their surfaces, respectively. More importantly, BKR on the U87 cell surfaces formed nanofibers in situ from nanoparticles and killed the cells. The bio-inspired morphology transformation of BKR peptide on the cell surfaces displays a great potential for cancer theranostics.

1.3 Summary and Outlook

In this review, recent progress of supramolecular self-assembled nanomaterials for fluorescence bioimaging was summarized. Supramolecular nanoassemblies as contrast agents have many advantages compared to small molecules, such as high stability, high sensitivity, and specificity. However, the preparation reliability of self-assembled nanomaterials is a key issue, which is due to the difficulty in controlling the supramolecular interactions. It is possible to transform the morphologies, structures, and corresponding fluorescence properties when encountering in biointerfaces with complicated physiological condition in vivo, ascribed to the dynamic nature of self-assembled nanomaterials.

For ex situ self-assembled nanomaterials, the dye-dispersed polymeric or semiconducting polymeric nanoparticles have been proven to be simple and effective supramolecular approach to construct nanoprobes/contrast agents for general fluorescence materials. The well-controlled nanomaterials with definite parameters such as size, shape, charge, payload, and surface chemistry are necessary for reliable application. The aggregation of fluorescence units should be precisely tuned to keep high fluorescence quantum yields by incorporating bulky groups, introducing moieties to induce intramolecular and intermolecular energy transfer. The AIE and J-type aggregation nanoparticles take advantage of fluorescence increase nature during aggregation process. For all the ex situ self-assembled nanomaterials, the stability is highly disable to face the complicated physiological conditions. They could meet the requirement of high-performance fluorescence contrast agents for clinical application.

On the other hand, the in situ self-assembly is much more interesting field that draws great attention from fundamental research. The in situ self-assembly can be intelligent to monitor the biological process, activity of biomolecules, and disease diagnosis in vivo. More importantly, in situ self-assembly is generally achieved under natural stimuli, such as enzyme, pH, and redox in specific physiological and pathological region. It will help the construction of nanoprobes or release of drugs effective in therapeutics and diagnostics due to the selective and efficient homing of material to specific tissues and biomolecular targets. For example, the in situ assembly showed long retention time, which was called aggregation-induced retention (AIR) effect, resulting in high performance of imaging and treatment. There is an extraordinary need of powerful new tools and strategies for characterizing the dynamics, morphology, and behavior of in situ self-assembled nanomaterials, which can identify their specific and useful physical properties from normal tissue. Furthermore, the design of sophisticated precursor for self-assembly would be a large challenge for the in situ assembly with fluorescence signal difference.

For all the self-assembled nanomaterials, further development bioimaging applications will be mainly focused on the FR/NIR emitters with narrow band emission. Various signal amplification strategies, such as FRET and metal-enhanced fluorescence, could be used to further improve their brightness for

fluorescence imaging. The biodistribution, such as liver and spleen, and their toxicity in vivo following systemic administration of self-assembled nanomaterials need to be evaluated through standardized, validated methods. Furthermore, the morphology and structure transformation followed by the disassembly and excretion of self-assembled nanomaterials in vivo should be paid great effort. The self-assembled nanomaterials with disassembility and degradability with high biocompatibility and low toxicity by systematically evaluation could be applied to clinical diagnostics and therapeutics of diseases. By collaboration with the multidisciplinary researchers from chemistry, biology, and medicine, we believe that the self-assembled nanomaterials will lead to benefits to all of us in the future.

References

1. Lehn J-M (1988) Supramolecular chemistry-scope and perspectives molecules, supermolecules, and molecular devices (Nobel Lecture). Angew Chem Int Ed 27(1):89–112
2. Li F, Lu J, Kong X, Hyeon T, Ling D (2017) Dynamic nanoparticle assemblies for biomedical applications. Adv Mater:1605897
3. Wang L, L-l Li, Y-s Fan, Wang H (2013) Host–guest supramolecular nanosystems for cancer diagnostics and therapeutics. Adv Mater 25(28):3888–3898
4. de Silva AP, Gunaratne HQN, Gunnlaugsson T, Huxley AJM, McCoy CP, Rademacher JT, Rice TE (1997) Signaling recognition events with fluorescent sensors and switches. Chem Rev 97(5):1515–1566
5. Michalet X, Pinaud FF, Bentolila LA, Tsay JM, Doose S, Li JJ, Sundaresan G, Wu AM, Gambhir SS, Weiss S (2005) Quantum dots for live cells, in vivo imaging, and diagnostics. Science 307(5709):538–544
6. de Chermont QlM, Chaneac C, Seguin J, Pelle F, Maitrejean S, Jolivet J-P, Gourier D, Bessodes M, Scherman D (2007) Nanoprobes with near-infrared persistent luminescence for in vivo imaging. Proc Natl Acad Sci USA 104(22):9266–9271
7. He S, Song B, Li D, Zhu C, Qi W, Wen Y, Wang L, Song S, Fang H, Fan C (2010) A graphene nanoprobe for rapid, sensitive, and multicolor fluorescent DNA analysis. Adv Funct Mater 20(3):453–459
8. Ding D, Li K, Liu B, Tang BZ (2013) Bioprobes based on AIE Fluorogens. Acc Chem Res 46(11):2441–2453
9. Bao B, Fan Q, Wang L, Huang W (2014) Recent advances in fluorescent conjugated polymer nanoparticles. Sci China Chem 44(3):282–294
10. Chen M, Yin M (2014) Design and development of fluorescent nanostructures for bioimaging. Prog Polym Sci 39(2):365–395
11. Razgulin A, Ma N, Rao J (2011) Strategies for in vivo imaging of enzyme activity: an overview and recent advances. Chem Soc Rev 40(7):4186–4216
12. Tao Z, Hong G, Shinji C, Chen C, Diao S, Antaris AL, Zhang B, Zou Y, Dai H (2013) Biological imaging using nanoparticles of small organic molecules with fluorescence emission at wavelengths longer than 1000 nm. Angew Chem Int Ed 52(49):13002–13006
13. Wu C, Schneider T, Zeigler M, Yu J, Schiro PG, Burnham DR, McNeill JD, Chiu DT (2010) Bioconjugation of ultrabright semiconducting polymer dots for specific cellular targeting. J Am Chem Soc 132(43):15410–15417
14. Peng HS, Stolwijk JA, Sun LN, Wegener J, Wolfbeis OS (2010) A nanogel for ratiometric fluorescent sensing of intracellular pH values. Angew Chem Int Ed 49(25):4246–4249
15. Wei H, Zhuo RX, Zhang XZ (2013) Design and development of polymeric micelles with cleavable links for intracellular drug delivery. Prog Polym Sci 38(3–4):503–535

16. Yin MZ, Shen J, Pisula W, Liang MH, Zhi LJ, Müllen K (2009) Functionalization of self-assembled hexa-peri-hexabenzocoronene fibers with peptides for bioprobing. J Am Chem Soc 131(41):14618–14619
17. Luo J, Lei T, Wang L, Ma YG, Cao Y, Wang J, Pei J (2009) Highly fluorescent rigid supramolecular polymeric nanowires constructed through multiple hydrogen bonds. J Am Chem Soc 131(6):2076–2077
18. Yin MZ, Feng CL, Shen J, Yu YM, Xu ZJ, Yang WT, Knoll W, Müllen K (2011) Dual-responsive interaction to detect DNA on template-based fluorescent nanotubes. Small 7 (12):1629–1634
19. Zhang D, Zhao Y-X, Qiao Z-Y, Mayerhöffer U, Spenst P, Li X-J, Würthner F, Wang H (2014) Nano-confined squaraine dye assemblies: new photoacoustic and near-infrared fluorescence dual-modular imaging probes in vivo. Bioconj Chem 25(11):2021–2029
20. Bunschoten A, Buckle T, Kuil J, Luker GD, Luker KE, Nieweg OE, van Leeuwen FWB (2012) Targeted non-covalent self-assembled nanoparticles based on human serum albumin. Biomaterials 33(3):867–875
21. Chen Q, Liang C, Wang X, He J, Li Y, Liu Z (2014) An albumin-based theranostic nano-agent for dual-modal imaging guided photothermal therapy to inhibit lymphatic metastasis of cancer post surgery. Biomaterials 35(34):9355–9362
22. Chen Q, Wang C, Zhan Z, He W, Cheng Z, Li Y, Liu Z (2014) Near-infrared dye bound albumin with separated imaging and therapy wavelength channels for imaging-guided photothermal therapy. Biomaterials 35(28):8206–8214
23. Sheng Z, Hu D, Zheng M, Zhao P, Liu H, Gao D, Gong P, Gao G, Zhang P, Ma Y, Cai L (2014) Smart human serum albumin-indocyanine green nanoparticles generated by programmed assembly for dual-modal imaging-guided cancer synergistic phototherapy. ACS Nano 8(12):12310–12322
24. Gao F-P, Lin Y-X, Li L-L, Liu Y, Mayerhoeffer U, Spenst P, Su J-G, Li J-Y, Würthner F, Wang H (2014) Supramolecular adducts of squaraine and protein for noninvasive tumor imaging and photothermal therapy in vivo. Biomaterials 35(3):1004–1014
25. Wu C, Hansen SJ, Hou Q, Yu J, Zeigler M, Jin Y, Burnham DR, McNeill JD, Olson JM, Chiu DT (2011) Design of highly emissive polymer dot bioconjugates for in vivo tumor targeting. Angew Chem Int Ed 50(15):3430–3434
26. Ye F, Wu C, Jin Y, Chan Y-H, Zhang X, Chiu DT (2011) Ratiometric temperature sensing with semiconducting polymer dots. J Am Chem Soc 133(21):8146–8149
27. Chan Y-H, Ye F, Gallina ME, Zhang X, Jin Y, Wu IC, Chiu DT (2012) Hybrid semiconducting polymer dot-quantum dot with narrow-band emission, near-infrared fluorescence, and high brightness. J Am Chem Soc 134(17):7309–7312
28. Yu J, Wu C, Zhang X, Ye F, Gallina ME, Rong Y, Wu IC, Sun W, Chan Y-H, Chiu DT (2012) Stable functionalization of small semiconducting polymer dots via covalent cross-linking and their application for specific cellular imaging. Adv Mater 24(26):3498–3504
29. Peng H-S, Chiu DT (2015) Soft fluorescent nanomaterials for biological and biomedical imaging. Chem Soc Rev 44(14):4699–4722
30. Xiong L, Shuhendler AJ, Rao J (2012) Self-luminescing BRET-FRET near-infrared dots for in vivo lymph-node mapping and tumour imaging. Nat Commun 3:1193
31. Shuhendler AJ, Pu K, Cui L, Uetrecht JP, Rao J (2014) Real-time imaging of oxidative and nitrosative stress in the liver of live animals for drug-toxicity testing. Nat Biotechnol 32 (4):373–380
32. Palner M, Pu K, Shao S, Rao J (2015) Semiconducting polymer nanoparticles with persistent near-infrared luminescence for in vivo optical imaging. Angew Chem Int Ed 54(39):11477–11480
33. Feng L, Zhu C, Yuan H, Liu L, Lv F, Wang S (2013) Conjugated polymer nanoparticles: preparation, properties, functionalization and biological applications. Chem Soc Rev 42 (16):6620–6633

34. Jeong K, Park S, Lee YD, Lim CK, Kim J, Chung BH, Kwon IC, Park CR, Kim S (2013) Conjugated polymer/photochromophore binary nanococktails: bistable photoswitching of near-infrared fluorescence for in vivo imaging. Adv Mater 25(39):5574–5580
35. Jin Y, Ye F, Zeigler M, Wu C, Chiu DT (2011) Near-infrared fluorescent dye-doped semiconducting polymer dots. ACS Nano 5(2):1468–1475
36. Danhier F, Ansorena E, Silva JM, Coco R, Le Breton A, Preat V (2012) PLGA-based nanoparticles: an overview of biomedical applications. J Control Release 161(2):505–522
37. Li K, Pan J, Feng SS, Wu AW, Pu KY, Liu YT, Liu B (2009) Generic strategy of preparing fluorescent conjugated-polymer-loaded poly(DL-lactide-co-glycolide) nanoparticles for targeted cell imaging. Adv Funct Mater 19(22):3535–3542
38. Li K, Liu YT, Pu KY, Feng SS, Zhan RY, Liu B (2011) Polyhedral oligomeric silsesquioxanes-containing conjugated polymer loaded PLGA nanoparticles with trastuzumab (herceptin) functionalization for HER2-positive cancer cell detection. Adv Funct Mater 21(2):287–294
39. Hong Y, Lam JWY, Tang BZ (2011) Aggregation-induced emission. Chem Soc Rev 40 (11):5361–5388
40. Qin A, Lam JWY, Tang BZ (2012) Luminogenic polymers with aggregation-induced emission characteristics. Prog Polym Sci 37(1):182–209
41. Hu R, Leung NLC, Tang BZ (2014) AIE macromolecules: syntheses, structures and functionalities. Chem Soc Rev 43(13):4494–4562
42. Mei J, Hong Y, Lam JWY, Qin A, Tang Y, Tang BZ (2014) Aggregation-induced emission: the whole is more brilliant than the parts. Adv Mater 26(31):5429–5479
43. Kwok RTK, Leung CWT, Lam JWY, Tang BZ (2015) Biosensing by luminogens with aggregation-induced emission characteristics. Chem Soc Rev 44(13):4228–4238
44. Liang J, Tang BZ, Liu B (2015) Specific light-up bioprobes based on AIEgen conjugates. Chem Soc Rev 44(10):2798–2811
45. Mei J, Leung NLC, Kwok RTK, Lam JWY, Tang BZ (2015) Aggregation-induced emission: together we shine, united we soar! Chem Rev 115(21):11718–11940
46. Wang H, Zhao E, Lam JWY, Tang BZ (2015) AIE luminogens: emission brightened by aggregation. Mater Today 18(7):365–377
47. Zhao Z, He B, Tang BZ (2015) Aggregation-induced emission of siloles. Chem Sci 6 (10):5347–5365
48. Yu Y, Feng C, Hong Y, Liu J, Chen S, Ng KM, Luo KQ, Tang BZ (2011) Cytophilic fluorescent bioprobes for long-term cell tracking. Adv Mater 23(29):3298–3302
49. Ma H, Qi C, Cheng C, Yang Z, Cao H, Yang Z, Tong J, Yao X, Lei Z (2016) AIE-active tetraphenylethylene cross-linked N-isopropylacrylamide polymer: a long-term fluorescent cellular tracker. ACS Appl Mater Interfaces 8(13):8341–8348
50. Wang Z, Chen S, Lam JWY, Qin W, Kwok RTK, Xie N, Hu Q, Tang BZ (2013) Long-term fluorescent cellular tracing by the aggregates of AIE bioconjugates. J Am Chem Soc 135 (22):8238–8245
51. Qin W, Ding D, Liu J, Yuan WZ, Hu Y, Liu B, Tang BZ (2012) Biocompatible nanoparticles with aggregation-induced emission characteristics as far-red/near-infrared fluorescent bioprobes for in vitro and in vivo imaging applications. Adv Funct Mater 22 (4):771–779
52. Ding D, Li K, Qin W, Zhan R, Hu Y, Liu J, Tang BZ, Liu B (2013) Conjugated polymer amplified far-red/near-infrared fluorescence from nanoparticles with aggregation-induced emission characteristics for targeted in vivo imaging. Adv Healthcare Mater 2(3):500–507
53. Li K, Jiang Y, Ding D, Zhang X, Liu Y, Hua J, Feng S-S, Liu B (2011) Folic acid-functionalized two-photon absorbing nanoparticles for targeted MCF-7 cancer cell imaging. Chem Commun 47(26):7323–7325
54. Li K, Qin W, Ding D, Tomczak N, Geng J, Liu R, Liu J, Zhang X, Liu H, Liu B, Tang BZ (2013) Photostable fluorescent organic dots with aggregation-induced emission (AIE dots) for noninvasive long-term cell tracing. Scientif Rep 3:1150

55. Qin W, Li K, Feng G, Li M, Yang Z, Liu B, Tang BZ (2014) Bright and photostable organic fluorescent dots with aggregation-induced emission characteristics for noninvasive long-term cell imaging. Adv Funct Mater 24(5):635–643
56. Gao Y, Feng G, Jiang T, Goh C, Ng L, Liu B, Li B, Yang L, Hua J, Tian H (2015) Biocompatible nanoparticles based on diketo-pyrrolo-pyrrole (DPP) with aggregation-induced red/NIR emission for in vivo two-photon fluorescence imaging. Adv Funct Mater 25(19):2857–2866
57. Shao A, Xie Y, Zhu S, Guo Z, Zhu S, Guo J, Shi P, James TD, Tian H, Zhu W-H (2015) Far-red and near-IR AIE-active fluorescent organic nanoprobes with enhanced tumor-targeting efficacy: shape-specific effects. Angew Chem Int Ed 54(25):7275–7280
58. Geng J, Goh CC, Qin W, Liu R, Tomczak N, Ng LG, Tangde BZ, Liu B (2015) Silica shelled and block copolymer encapsulated red-emissive AIE nanoparticles with 50% quantum yield for two-photon excited vascular imaging. Chem Commun 51(69):13416–13419
59. Geng J, Li K, Ding D, Zhang X, Qin W, Liu J, Tang BZ, Liu B (2012) Lipid-PEG-folate encapsulated nanoparticles with aggregation induced emission characteristics: cellular uptake mechanism and two-photon fluorescence imaging. Small 8(23):3655–3663
60. Ding D, Goh CC, Feng G, Zhao Z, Liu J, Liu R, Tomczak N, Geng J, Tang BZ, Ng LG, Liu B (2013) Ultrabright organic dots with aggregation-induced emission characteristics for real-time two-photon intravital vasculature imaging. Adv Mater 25(42):6083–6088
61. Kaiser TE, Wang H, Stepanenko V, Würthner F (2007) Supramolecular construction of fluorescent J-aggregates based on hydrogen-bonded perylene dyes. Angew Chem Int Ed 46 (29):5541–5544
62. Wang H, Kaiser TE, Uernura S, Würthner F (2008) Perylene bisimide J-aggregates with absorption maxima in the NIR. Chem Commun 10:1181–1183
63. Wang L, Li W, Lu J, Zhao Y-X, Fan G, Zhang J-P, Wang H (2013) Supramolecular nano-aggregates based on bis(pyrene) derivatives for lysosome-targeted cell imaging. J Phys Chem C 117(50):26811–26820
64. Yang P-P, Yang Y, Gao Y-J, Wang Y, Zhang J-C, Lin Y-X, Dai L, Li J, Wang L, Wang H (2015) Unprecedentedly high tissue penetration capability of co-assembled nanosystems for two-photon fluorescence imaging in vivo. Adv Optical Mater 3(5):646–651
65. Olivier J-H, Widmaier J, Ziessel R (2011) Near-infrared fluorescent nanoparticles formed by self-assembly of lipidic (bodipy) dyes. Chem Eur J 17(42):11709–11714
66. Choi S, Bouffard J, Kim Y (2014) Aggregation-induced emission enhancement of a meso-trifluoromethyl BODIPY via J-aggregation. Chem Sci 5(2):751–755
67. Xu Z, Liao Q, Wu Y, Ren W, Li W, Liu L, Wang S, Gu Z, Zhang H, Fu H (2012) Water-miscible organic J-aggregate nanoparticles as efficient two-photon fluorescent nano-probes for bio-imaging. J Mater Chem 22(34):17737–17743
68. Hayashi T, Hamachi I (2012) Traceless affinity labeling of endogenous proteins for functional analysis in living cells. Acc Chem Res 45(9):1460–1469
69. Kubota R, Hamachi I (2015) Protein recognition using synthetic small-molecular binders toward optical protein sensing in vitro and in live cells. Chem Soc Rev 44(13):4454–4471
70. Takaoka Y, Ojida A, Hamachi I (2013) Protein organic chemistry and applications for labeling and engineering in live-cell systems. Angew Chem Int Ed 52(15):4088–4106
71. Mizusawa K, Takaoka Y, Hamachi I (2012) Specific cell surface protein imaging by extended self-assembling fluorescent turn-on nanoprobes. J Am Chem Soc 134(32):13386–13395
72. Fan G, Lin Y-X, Yang L, Gao F-P, Zhao Y-X, Qiao Z-Y, Zhao Q, Fan Y-S, Chen Z, Wang H (2015) Co-self-assembled nanoaggregates of BODIPY amphiphiles for dual colour imaging of live cells. Chem Commun 51(62):12447–12450
73. Qiao Z-Y, Hou C-Y, Zhao W-J, Zhang D, Yang P-P, Wang L, Wang H (2015) Synthesis of self-reporting polymeric nanoparticles for in situ monitoring of endocytic microenvironmental pH. Chem Commun 51(63):12609–12612

74. Raghupathi KR, Guo J, Munkhbat O, Rangadurai P, Thayumanavan S (2014) Supramolecular disassembly of facially amphiphilic dendrimer assemblies in response to physical, chemical, and biological stimuli. Acc Chem Res 47(7):2200–2211
75. Amado Torres D, Garzoni M, Subrahmanyam AV, Pavan GM, Thayumanavan S (2014) Protein-triggered supramolecular disassembly: insights based on variations in ligand location in amphiphilic dendrons. J Am Chem Soc 136(14):5385–5399
76. Wang H, Zhuang J, Raghupathi KR, Thayumanavan S (2015) A supramolecular dissociation strategy for protein sensing. Chem Commun 51(97):17265–17268
77. Gao Y, Shi J, Yuan D, Xu B (2012) Imaging enzyme-triggered self-assembly of small molecules inside live cells. Nat Commun 3:1033
78. Gao Y, Berciu C, Kuang Y, Shi J, Nicastro D, Xu B (2013) Probing nanoscale self-assembly of nonfluorescent small molecules inside live mammalian cells. ACS Nano 7(10):9055–9063
79. Dragulescu-Andrasi A, Kothapalli S-R, Tikhomirov GA, Rao J, Gambhir SS (2013) Activatable oligomerizable imaging agents for photoacoustic imaging of furin-like activity in living subjects. J Am Chem Soc 135(30):11015–11022
80. Liang G, Ren H, Rao J (2010) A biocompatible condensation reaction for controlled assembly of nanostructures in living cells. Nat Chem 2(1):54–60
81. Ye D, Shuhendler AJ, Cui L, Tong L, Tee SS, Tikhomirov G, Felsher DW, Rao J (2014) Bioorthogonal cyclization-mediated in situ self-assembly of small-moleculeprobes for imaging caspase activity in vivo. Nat Chem 6(6):519–526
82. Ye D, Shuhendler AJ, Pandit P, Brewer KD, Tee SS, Cui L, Tikhomirov G, Rutt B, Rao J (2014) Caspase-responsive smart gadolinium-based contrast agent for magnetic resonance imaging of drug-induced apoptosis. Chem Sci 5(10):3845–3852
83. Shi H, Kwok RTK, Liu J, Xing B, Tang BZ, Liu B (2012) Real-time monitoring of cell apoptosis and drug screening using fluorescent light-up probe with aggregation-induced emission characteristics. J Am Chem Soc 134(43):17972–17981
84. Yuan Y, Kwok RTK, Tang BZ, Liu B (2014) Targeted theranostic platinum (IV) prodrug with a built-in aggregation-induced emission light-up apoptosis sensor for noninvasive early evaluation of its therapeutic responses in situ. J Am Chem Soc 136(6):2546–2554
85. Han H, Jin Q, Wang Y, Chen Y, Ji J (2015) The rational design of a gemcitabine prodrug with AIE-based intracellular light-up characteristics for selective suppression of pancreatic cancer cells. Chem Commun 51(98):17435–17438
86. Yuan Y, Zhang C-J, Gao M, Zhang R, Tang BZ, Liu B (2015) Specific light-up bioprobe with aggregation-induced emission and activatable photoactivity for the targeted and image-guided photodynamic ablation of cancer cells. Angew Chem Int Ed 54(6):1780–1786
87. Liang J, Kwok RTK, Shi H, Tang BZ, Liu B (2013) Fluorescent light-up probe with aggregation-induced emission characteristics for alkaline phosphatase sensing and activity study. ACS Appl Mater Interfaces 5(17):8784–8789
88. Duan Z, Gao Y-J, Qiao Z-Y, Qiao S, Wang Y, Hou C, Wang L, Wang H (2015) pH-Sensitive polymer assisted self-aggregation of bis(pyrene) in living cells in situ with turn-on fluorescence. Nanotechnology 26(35)
89. Lin Y-X, Qiao S-L, Wang Y, Zhang R-X, An H-W, Ma Y, Rajapaksha RPYJ, Qiao Z-Y, Wang L, Wang H (2017) An in situ intracellular self-assembly strategy for quantitatively and temporally monitoring autophagy. ACS Nano 11(2):1826–1839
90. Carter NA, Grove TZ (2015) Repeat-proteins films exhibit hierarchical anisotropic mechanical properties. Biomacromol 16(3):706–714
91. Feldkamp U, Niemeyer CM (2006) Rational design of DNA nanoarchitectures. Angew Chem Int Ed 45(12):1856–1876
92. Callmann CE, Barback CV, Thompson MP, Hall DJ, Mattrey RF, Gianneschi NC (2015) Therapeutic enzyme-responsive nanoparticles for targeted delivery and accumulation in tumors. Adv Mater 27(31):4611–4615
93. Nguyen MM, Carlini AS, Chien M-P, Sonnenberg S, Luo C, Braden RL, Osborn KG, Li Y, Gianneschi NC, Christman KL (2015) Enzyme-responsive nanoparticles for targeted

accumulation and prolonged retention in heart tissue after myocardial infarction. Adv Mater 27(37):5547–5552
94. Moyer TJ, Finbloom JA, Chen F, Toft DJ, Cryns VL, Stupp SI (2014) pH and amphiphilic structure direct supramolecular behavior in biofunctional assemblies. J Am Chem Soc 136 (42):14746–14752
95. Matson JB, Navon Y, Bitton R, Stupp SI (2015) Light-controlled hierarchical self-assembly of polyelectrolytes and supramolecular polymers. ACS Macro Lett 4(1):43–47
96. Sun H-L, Chen Y, Zhao J, Liu Y (2015) Photocontrolled reversible conversion of nanotube and nanoparticle mediated by -cyclodextrin dimers. Angew Chem Int Ed 54(32):9376–9380
97. Shao H, Parquette JR (2009) Controllable peptide-dendron self-assembly: interconversion of nanotubes and fibrillar nanostructures. Angew Chem Int Ed 48(14):2525–2528
98. An H-W, Qiao S-L, Li L-L, Yang C, Lin Y-X, Wang Y, Qao Z-Y, Wang L, Wang H (2016) Bio-orthogonally Deciphered binary nanoemitters for tumor diagnostics. ACS Appl Mater Interfaces 8(30):19202–19207
99. Yang P-P, Zhao X-X, Xu A-P, Wang L, Wang H (2016) Reorganization of self-assembled supramolecular materials controlled by hydrogen bonding and hydrophilic-lipophilic balance. J Mater Chem B 4(15):2662–2668
100. Esler WP, Stimson ER, Ghilardi JR, Lu Y-A, Felix AM, Vinters HV, Mantyh PW, Lee JP, Maggio JE (1996) Point substitution in the central hydrophobic cluster of a human β-Amyloid congener disrupts peptide folding and abolishes plaque competence. Biochemistry 35(44):13914–13921
101. Molla MR, Prasad P, Thayumanavan S (2015) Protein-induced supramolecular disassembly of amphiphilic polypeptide nanoassemblies. J Am Chem Soc 137(23):7286–7289
102. Xu A-P, Yang P-P, Yang C, Gao Y-J, Zhao X-X, Luo Q, Li X-D, Li L-Z, Wang L, Wang H (2016) Bio-inspired metal ions regulate the structure evolution of self-assembled peptide-based nanoparticles. Nanoscale 8(29):14078–14083
103. Yu YP, Wang Q, Liu YC, Xie Y (2014) Molecular basis for the targeted binding of RGD-containing peptide to integrin αvβ3. Biomaterials 35(5):1667–1675
104. Craig D, Gao M, Schulten K, Vogel V (2004) Structural insights into how the MIDAS ion stabilizes integrin binding to an RGD peptide under force. Structure 12(11):2049–2058
105. Puklin-Faucher E, Vogel V (2009) Integrin activation dynamics between the RGD-binding site and the headpiece hinge. J Biol Chem 284(52):36557–36568